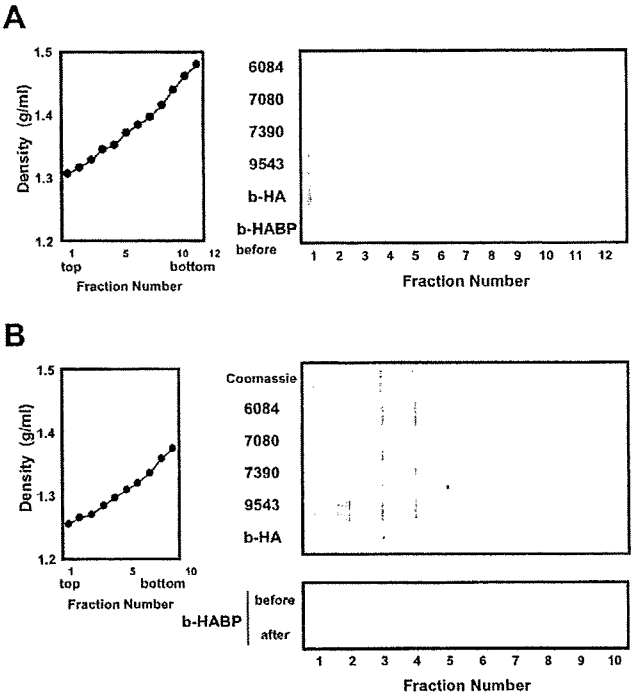


FIGURE 6. CsCl density gradient centrifugation of the void fraction of extracts of chicken ciliary bodies after gel-filtration chromatography. (A) Analysis after CsCl density gradient centrifugation with an initial density of 1.37 g/mL. The top fraction shows positive reactions with all the versican and fibrillin-1 antibodies as well as b-HABP. (B) Analysis after CsCl density gradient centrifugation with an initial density of 1.30 g/mL. The top fraction shown in (A) was analyzed by slot-blot after CsCl density gradient centrifugation. Fractions 3 to 5 showed positive reactions with the antibodies. There was faint b-HABP staining in fractions 3 to 4 before alkaline treatment, whereas strong reactivity was observed in these fractions after alkaline treatment.

When the samples after CsCl density gradient centrifugation (fractions under 4 M guanidine HCl) were subjected to slot blot analysis, vitreous body microfibrils did not react with antibodies against the hyaluronan-binding region of versican or with

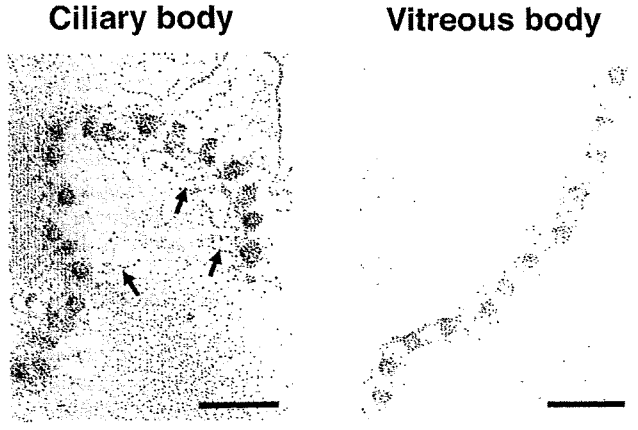


FIGURE 7. Visualization of versican-bound microfibrils from chicken ciliary and vitreous bodies by rotary shadowing electron microscopy. The ciliary body and vitreous body fractions around 1.29 g/mL after CsCl density gradient centrifugation showed the multiple beads and strings structure characteristic of microfibrils.[20] The ciliary body sample shows additional projections (*arrows*) around the basic structure. Bar, 100 nm.

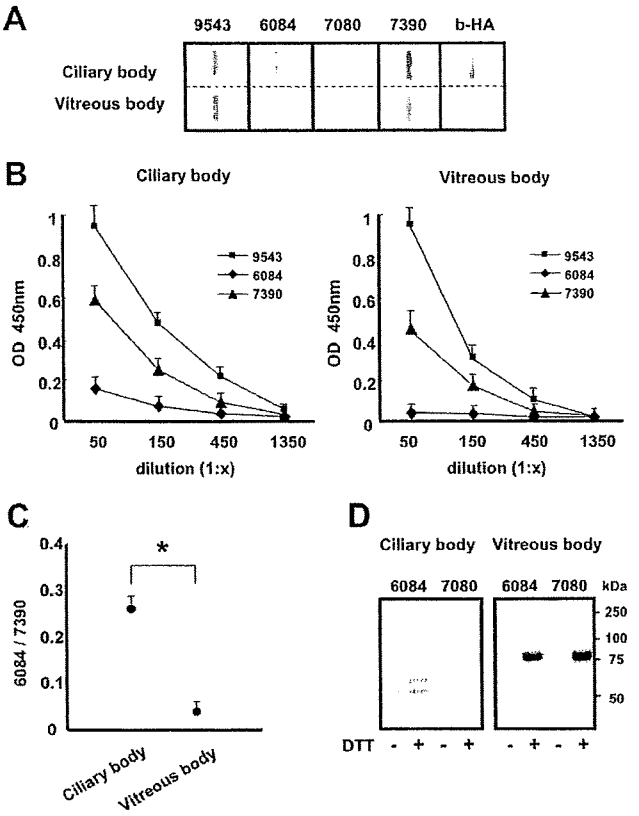


FIGURE 8. Comparison of versican-bound fibrillin microfibrils extracted from chicken ciliary and vitreous bodies. (A) Slot-blot analyses of samples after CsCl density gradient centrifugation with fibrillin-1 and versican antibodies and b-HA. Both the amino terminus of versican and hyaluronan-binding activity were detected in the ciliary body sample, indicating that the structure shown in Figure 7, the ciliary body, contains FiVerHy complexes, but that vitreous body samples do not, suggesting that the amino terminus of versican is cleaved in versican-bound microfibrils present in the vitreous body. Both samples were adjusted to react equally with polyclonal antibody 9543. (B) ELISA analyses with fibrillin-1 and versican antibodies. Reactivity of 6084 with vitreous body samples was hardly detected in all dilutions. (C) Comparison of the ratios of antibody reactivity of the amino and carboxyl termini of versican. The ratio of reactivity of antibodies 6084 to 7390 was significantly small in the vitreous body in comparison with the ciliary body. Data are the mean ± SE ($n = 3$). *$P < 0.0001$. (D) Western blot analyses with antibodies against the amino terminus of versican, performed on extracts from chicken ciliary body and vitreous body, with or without DTT. The distinct 80-kDa fragment was not detected in the absence of DTT, but was detected in the presence of reducing conditions with DTT in extracts of vitreous bodies.

b-HA (Fig. 8A). By contrast, ciliary body microfibrils showed reactivity to 6084 and 7080 antibodies and a binding affinity for hyaluronan. All samples examined reacted with the antibodies against fibrillin-1 and the carboxyl-terminus of versican. The same fractions were studied by ELISA (Fig. 8B). The vitreous body sample reacted negatively with 6084 in all dilutions. The ratio of 6084 to 7390 in dilution 1:50 was significantly small in vitreous body comparison with ciliary body (Fig. 8C; $P < 0.0001$). We detected a distinct 80-kDa band reactive to 6084 and 7080 antibodies but not reactive to 7390 antibodies in the vitreous samples under reducing conditions with DTT by Western blot study (Fig. 8D, and data not shown). This 80-kDa fragment was not detected in samples derived from ciliary bodies, regardless of the presence or absence of DTT, whereas some degraded bands were seen in each lane (Fig. 8D). This finding suggests that ciliary bodies are mainly equipped with

the entire FiVerHy complex, which remains in the stacking gel. Amino acid sequence analysis of this 80-kDa band revealed an N-terminal peptide KKTLVKG, which is identical with the amino terminus of chicken versican.

Reactivity of 7080 with ciliary and vitreous bodies was absent in ELISA analysis (data not shown). We think that this is due to masking of the epitope by the loop structure of versican, which is not present in the blot, but is present in the fluid, as the antibodies were specifically raised against the hyaluronan-binding region near the disulfide bonds.

## Discussion

Comparisons of the amino acid sequences used for preparing antibodies 7080 and 7390 with the respective chick regions by BLAST searches revealed identities of 50% and 93%, respectively. These moderate and high similarities of the amino acid sequences allowed for cross-reactivity of the antibodies with the corresponding chicken sequences, thereby enabling us to perform these studies on chick samples. In addition, these antibodies showed staining patterns for versican in chick retinal samples similar to those shown previously[17] by immunohistochemical and Western blot analyses (data not shown). There is a possibility that these antibodies also react with chicken aggrecan. However, an anti-aggrecan antibody (Santa Cruz Biotechnology Inc., Santa Cruz, CA) showed no staining of human, mouse, and rat ciliary bodies (data not shown). Therefore, our newly prepared polyclonal antibodies appeared to react well with chicken versican in the tissues examined.

We found intense reactivity to b-HA in the low-molecular-weight fractions from 29 to 33 after gel filtration chromatography, but the fractions showed only faint reactivity with b-HABP. These fractions showed relatively stronger reactions with antibodies 6084 and 7080 than with antibody 7390, suggesting that they may contain a fragment corresponding to the hyaluronan-binding region of versican that is not bound to hyaluronan.

Versican of the FiVerHy complex in vitreous samples releases gigantic hyaluronan because of the split of disulfide bond in hyaluronan-binding region of versican under the reducing conditions, and it may enable the 80 kDa of amino terminus versican fragment to enter the running gels as shown in Figure 8D. The 80-kDa fragment we observed in the chicken vitreous body may correspond to the 55 kDa of amino terminal versican fragment detected in the bovine vitreous body.[22] In extracts from brain, a fragment corresponding to the hyaluronan-binding region of versican has been also reported.[30] Some proteolytic reactions may be involved in these processes. Taken together, the present data allow us to propose the hypothesis that the hyaluronan-binding region of versican in the vitreous body is cleaved from the FiVerHy complex in the ciliary body. We estimate that this may be reflected in the different forms of microfibrils in the vitreous body, detected by rotary shadowing electron microscopy, which could be distinguished from the FiVerHy form in the ciliary body (Fig. 7).

In most patients with Wagner syndrome, an optically empty vitreous cavity, secondary vitreous body degeneration and a preretinal avascular membrane are the initial clinical presentations. Recent studies have identified novel mutations of the CSPG2/versican gene in Wagner syndrome that result in abnormal structures or balance shifts of chondroitin sulfate–attachment region $\beta$.[31–33] Loss of an important proteolytic cleavage site in chondroitin sulfate attachment region $\beta$, due to these mutations might be the trigger of the vitreous body obstructions in this syndrome, since these abnormal FiVerHy complexes may result in different physiological properties there.

The real-time PCR analysis showed that V0 and V1 are the major isoforms in the ciliary body. It suggests that abundant chondroitin sulfates are required in this tissue. An appropriate balance of each splice isoform may be important for regulation of chondroitin sulfates. Hence, an imbalance of splice variants may result in ocular disorders such as Wagner disease and erosive vitreoretinopathy.[33]

We previously tried immunoprecipitation to purify the FiVerHy complex by using 7080, 6084, and 7390 antibodies, but all failed. We speculate that the cause of these failures is because the complex is too gigantic. Indeed, the FiVerHy complex eluted in the void fractions as shown in Figure 5. In addition, maybe for the same reason, hyaluronan affinity columns are not suitable for purification of this complex. Further, hyaluronan affinity columns are not suitable as the purifying sample also includes hyaluronan in the complex, which may competitively affect their affinity. We also failed to separate the sample by electrophoresis for Western blot analysis, as the complex had such a high molecular weight that it remained trapped at the top of the gel. Thus, we came to the present approach for purification.

Our previous report showed that monomeric versican eluted in the middle fractions of sieve chromatography with Sepharose CL-2B.[15] In this study, versican from the ciliary body sample eluted in the void volume, rather than in the middle of the sieved materials. This result suggests that most of the versican is bound to microfibrils and forms huge complexes with hyaluronan. Association of the complex in the presence of 4 M guanidine HCl further suggests the presence of strong linkages, such as covalent bonds, among versican, fibrillin-1, and hyaluronan.

Our slot-blotting results, shown in Figure 6B, suggest that the FiVerHy complex is mainly composed of proteins, because it had a density of ~1.29 g/mL. Although the fractions around 1.29 g/mL strongly reacted with the antibodies, they hardly reacted with b-HABP before alkaline treatment. However, the samples on the membrane reacted strongly with b-HABP after alkaline treatment (Fig. 6B, fractions 3 and 4), suggesting that some protein constituents of the FiVerHy complex may prohibit the exposure of hyaluronan.

The anti-proteoglycan ΔDi-6S and ΔDi-4S antibodies showed no staining in ciliary zonules but detected immunoreactivity in the nonpigmented epithelium. This finding may suggest that the regions involved in the attachment of chondroitin sulfate to the aminoterminal end of versican are shed into the vitreous body and that only the carboxyl-terminal end of versican bound to fibrillin microfibrils accumulates in ciliary zonules. The flexibility and water-content property of integrant FiVerHy complex in the ciliary body may be essential for accommodation and aqueous humor secretion, respectively. The mobility of hyaluronan accompanied with chondroitin sulfate shed into the vitreous body, being free from behavioral restriction by fibrillin-1 attached to the carboxyl terminus of versican, may be also significant for it to accomplish its physiological function there.

Exfoliation syndrome (XFS) is an age-related disorder that constitutes the most common identifiable cause of glaucoma. The hallmark of the disease is the pathologic production and accumulation of an abnormal fibrillar exfoliation material (XFM) in many ocular tissues. Ultrastructural evidence suggests that XFM is mainly produced by epithelial cells of the iris, ciliary body, and lens. Of interest, Ovodenko et al.[34] identified both fibullin-1 and versican in XFM, and genome-wide scan of XFS suggested the involvement of fibrillin-1, MMP-2, and TIMP-1.[35] Thus, FiVerHy complex as well as the proteolytic enzymes and the inhibitors may be components of the molecular background of XFS.

## *References*


1. Allingham RR, Damji KF, Freedman S, Moroi SE, Shafranov G, Shields MB. *Shields' Textbook of Glaucoma.* 5th ed. Philadelphia: Lippincott Williams and Wilkins; 2005:5–35.
2. Forrester JV. *The Eye Basic Sciences in Practice.* 2nd ed. New York: WB Saunders; 2002:29–37.
3. James J. *Ophthalmology.* 2nd ed. St. Louis: Mosby; 2004:1113–1114.
4. Schmut O. The organization of tissues of the eye by different collagen types. *Albrecht Von Graefes Arch Klin Exp Ophthalmol.* 1978;207:189–199.
5. Marshall GE, Konstas AG, Abraham S, Lee WR. Extracellular matrix in aged human ciliary body: an immunoelectron microscope study. *Invest Ophthalmol Vis Sci.* 1992;33:2546–2560.
6. Rittig M, Lütjen-Drecoll E, Rauterberg J, Jander R, Mollenhauer J. Type-VI collagen in the human iris and ciliary body. *Cell Tissue Res.* 1990;259:305–312.
7. Streeten BW, Licari PA. The zonules and the elastic microfibrillar system in the ciliary body. *Invest Ophthalmol Vis Sci.* 1983;24:667–681.
8. Schlotzer-Schrehardt U, von der Mark K, Sakai LY, Naumann GO. Increased extracellular deposition of fibrillin-containing fibrils in pseudoexfoliation syndrome. *Invest Ophthalmol Vis Sci.* 1997;38:970–984.
9. Tamm E, Baur A, Lütjen-Drecoll E. Synthesis of extracellular matrix components by human ciliary muscle cells in culture. *Curr Eye Res.* 1992;11:333–341.
10. Sakai LY, Keene DR, Engvall E. Fibrillin, a new 350-kD glycoprotein, is a component of extracellular microfibrils. *J Cell Biol.* 1986;103:2499–2509.
11. Ashworth JL, Kielty CM, McLeod D. Fibrillin and the eye. *Br J Ophthalmol.* 2000;84:1312–1317.
12. Ren ZX, Brewton RG, Mayne R. An analysis by rotary shadowing of the structure of the mammalian vitreous humor and zonular apparatus. *J Struct Biol.* 1991;106:57–63.
13. Corson GM, Charbonneau NL, Keene DR, Sakai LY. Differential expression of fibrillin-3 adds to microfibril variety in human and avian, but not rodent, connective tissues. *Genomics.* 2004;83:461–472.
14. Dietz HC, Cutting GR, Pyeritz RE, et al. Marfan syndrome caused by a recurrent de novo missense mutation in the fibrillin gene. *Nature.* 1991;352:337–339.
15. Kimata K, Oike Y, Tani K, et al. A large chondroitin sulfate proteoglycan (PG-M) synthesized before chondrogenesis in the limb bud of chick embryo. *J Biol Chem.* 1986;261:13517–13525.
16. Zako M, Shinomura T, Kimata K. Alternative splicing of the unique "PLUS" domain of chicken PG-M/versican is developmentally regulated. *J Biol Chem.* 1997;272:9325–9331.
17. Zako M, Shinomura T, Miyaishi O, Iwaki M, Kimata K. Transient expression of PG-M/versican, a large chondroitin sulfate proteoglycan in developing chicken retina. *J Neurochem.* 1997;69:2155–2161.
18. Zhao X, Russell P. Versican splice variants in human trabecular meshwork and ciliary muscle. *Mol Vis.* 2005;11:603–608.
19. Ueda J, Yue BY. Distribution of myocilin and extracellular matrix components in the corneoscleral meshwork of human eyes. *Invest Ophthalmol Vis Sci.* 2003;44:4772–4779.
20. Isogai Z, Aspberg A, Keene DR, Ono RN, Reinhardt DP, Sakai LY. Versican interacts with fibrillin-1 and links extracellular microfibrils to other connective tissue networks. *J Biol Chem.* 2002;277:4565–4572.
21. Chan FL, Choi HL, Underhill CB. Hyaluronan and chondroitin sulfate proteoglycans are colocalized to the ciliary zonule of the rat eye: a histochemical and immunocytochemical study. *Histochem Cell Biol.* 1997;107:289–301.
22. Reardon A, Heinegard D, McLeod D, Sheehan JK, Bishop PN. The large chondroitin sulphate proteoglycan versican in mammalian vitreous. *Matrix Biol.* 1998;17:325–333.
23. Bishop PN. Structural macromolecules and supramolecular organisation of the vitreous gel. *Prog Retin Eye Res.* 2000;19:323–344.
24. Hasegawa K, Yoneda M, Kuwabara H, et al. Versican, a major hyaluronan-binding component in the dermis, loses its hyaluronan-binding ability in solar elastosis. *J Invest Dermatol.* 2007;127:1657–1663.
25. Isogai Z, Ono RN, Ushiro S, et al. Latent transforming growth factor beta-binding protein 1 interacts with fibrillin and is a microfibril-associated protein. *J Biol Chem.* 2003;278:2750–2757.
26. Isogai Z, Shinomura T, Yamakawa N, et al. 2B1 antigen characteristically expressed on extracellular matrices of human malignant tumors is a large chondroitin sulfate proteoglycan, PG-M/versican. *Cancer Res.* 1996;56:3902–3908.
27. Inoue Y, Yoneda M, Zhao J, et al. Molecular cloning and characterization of chick SPACRCAN. *J Biol Chem.* 2006;281:10381–10388.
28. Yoneda M, Suzuki S, Kimata K. Hyaluronic acid associated with the surfaces of cultured fibroblasts is linked to a serum-derived 85-kDa protein. *J Biol Chem.* 1990;265:5247–5257.
29. Morris NP, Keene DR, Glanville RW, Bentz H, Burgeson RE. The tissue form of type VII collagen is an antiparallel dimer. *J Biol Chem.* 1986;261:5638–5644.
30. Westling J, Gottschall PE, Thompson VP, et al. ADAMTS4 (aggrecanase-1) cleaves human brain versican V2 at Glu405-Gln406 to generate glial hyaluronate binding protein. *Biochem J.* 2004;377:787–795.
31. Miyamoto T, Inoue H, Sakamoto Y, et al. Identification of a novel splice site mutation of the CSPG2 gene in a Japanese family with Wagner syndrome. *Invest Ophthalmol Vis Sci.* 2005;46:2726–2735.
32. Kloeckener-Gruissem B, Bartholdi D, Abdou MT, Zimmermann DR, Berger W. Identification of the genetic defect in the original Wagner syndrome family. *Mol Vis.* 2006;12:350–355.
33. Mukhopadhyay A, Nikopoulos K, Maugeri A, et al. Erosive vitreoretinopathy and Wagner disease are caused by intronic mutations in CSPG2/Versican that result in an imbalance of splice variants. *Invest Ophthalmol Vis Sci.* 2006;47:3565–3572.
34. Ovodenko B, Rostagno A, Neubert TA, et al. Proteomic analysis of exfoliation deposits. *Invest Ophthalmol Vis Sci.* 2007;48:1447–1457.
35. Lemmela S, Forsman E, Sistonen P, Eriksson A, Forsius H, Jarvela I. Genome-wide scan of exfoliation syndrome. *Invest Ophthalmol Vis Sci.* 2007;48:4136–4142.

# 高齢者医療の中での褥瘡

磯貝　善蔵
（国立長寿医療センター先端医療部先端薬物療法科）

ここ国立長寿医療センターは，2004年3月に高齢者医療に関するさまざまな問題を解決していくために，愛知県に設立されたわが国で6番目のナショナルセンターです．皮膚科医として着任した私に与えられた主要課題は褥瘡でありまして，ここでの褥瘡の診療と管理，研究を任されることになりました．それまでは褥瘡診療に関して多くの経験はなく，むしろ膠原病や血管炎の診療を中心にしていましたが，このセンターのさまざまなスタッフに協力していただき，一歩ずつ勉強していきました．褥瘡に詳しい薬剤師の古田勝経副薬剤部長のご協力が支えになりました．

しかし褥瘡診療を勉強していく過程においては驚くことばかりでした．学会に参加してみても褥瘡に関する診療体系が確立されておらず，ラップ療法などのさまざまな方法が医療現場で行われている状況です．さらにチーム医療といっても診療に参加する職種もさまざまで，医師の役割と責任の所在も曖昧に感じました．また高齢者医療では社会的な要素が大きく関与するため，患者さんの個別性が強く標準化しにくいと感じました．褥瘡医療の現場は必死ではあるのですが，治癒や改善という結果が出なければ精神的に疲弊することになります．そこで自分の置かれた立場である病院皮膚科医であり研究機関勤務としての立場を最大限活かして，褥瘡医療の問題を解決していこうとしました．

第一に病院皮膚科医としての褥瘡への取り組み方を工夫しました．高齢者はさまざまな臓器に疾患を抱えており，包括的な診療と専門的な診療を上手に使い分けることが求められています．皮膚科医は包括的な視点と局所的な視点をバランスよく使い分けることができるので，高齢者に対する良質な病院医療を行ううえで重要な職種と思います．病院皮膚科医は他科医師のみならず薬剤師，看護師，理学療法師，ソーシャルワーカーなどとの情報交換や相談をする機会がとても多く，彼らは病院皮膚科医の理解者，協力者です．たとえば褥瘡医療に重要な患者さんの併存疾患の予後や安定性，リハビリテーション，看護上の問題点，薬剤や創傷被覆剤の種類や使用法，退院後の医療，介護サービスの相談などは彼らとの有機的なつながりをもち，かつ皮膚科医の責任をもって行っていきました．私にとっては退院支援会議への出席や地域の一般医との交流も高齢者を取り巻く医療体制を学ぶためのよい機会でした．その上に立って褥瘡対策チームの医師がきちんとイニシアチブをとる褥瘡対策チームを構築していきました．

診療上心がけたのは，日常診療の中で褥瘡の本質を細かに観察することでした．処置はいわば分割された手術であるにも関わらず，現在まであまり研究されていませんでした．しかし，現場の高齢の褥瘡患者さんやその家族は，できれば処置で治癒することを切に望んでいます．処置の意味を考えながら毎日変化する褥瘡の臨床を診療するのは，病院皮膚科医の義務であるとともに醍醐味であると思います．

研究機関勤務としてはセンター内の運動器疾患研究部と医療工学研究部，そして群馬大学皮膚科，愛知県立看護大学との共同研究を通して褥瘡の疾患としての研究を行っています．褥瘡は医師の関心が十分ではなく，現行の保険診療制度と病院皮膚科医の相対的不足の中で皮膚疾患としての研究の側面が不十分で，むしろケアの延長として看護領域で注目されてきました．しかしながら，褥瘡はしばしば重症の感染性皮膚潰瘍となり，生命予後的にも患者さんや家族の苦痛としても重大な疾患です．疾患としての研究においてはまず褥瘡を疾患レベルまで引き上げることを目標に臨床的，基礎的なアプローチを行ってきました．そのためには疾患をもつ患者さんを治療する現場が大切で，現場からの問題点をどのように研究に翻訳するかを考えてきました．

わが国での医療を支えてきたのは使命感と責任感のある現場医療者であり，昨今いわれている医療崩壊は現場力の低下であるといわれています．褥瘡は多大な現場のチーム力が必要な疾患であり，現場に携わる病院皮膚科医の力量が求められるとともに，その力を最大限発揮できる疾患と感じています．

# 褥　瘡

## 1 定義

体への外力は骨と皮膚表層間の軟部組織の血流を低下、停止させる。これが一定期間持続され、組織が阻血性障害になり発症する皮膚潰瘍である。

## 2 施設基準としての褥瘡対策

厚生労働省によって平成14年に病院に対する褥瘡対策未実施減算が導入され、対策をおこなわなければ全ての入院患者の入院基本料を減算することになって、褥瘡への関心が高まった。平成18年度からは減算は廃止され、入院基本料算定の必要用件として院内の褥瘡対策が求められている。

## 3 褥瘡の予防

自立度の低い患者や褥瘡に関する危険因子を有する患者は予防対策を講じることが必要である。厚生労働省から褥瘡の診療計画書の例が示されている（文献1）。その中でも基本的動作能力と病的骨突出が重要である。その評価に応じて体圧分散寝具を適切に使用する。エアマットレスは寝返りがうてない患者の褥瘡予防には最も有用である。最近では自動で除圧機能を持っている高機能エアマットレスも発売されているが、時にずれ力を発生させることもある。体動のできる患者ではエアマットレスは不快であり、転倒などの危険も高くなるので通常ウレタンフォームマットレスが適応になる。危険因子のある患者では骨突出部位が褥瘡の好発部位であるのでこまめに観察する。看護師が排泄ケアと同時におこなうことが効率的であり、軽症のうちに発見することが重要である。

## 4 褥瘡が発見されたら

褥瘡の部位と重症度を把握し、次に発症した原因を考える。

1）重症度評価：

図のように急性期とそれ以降、浅い褥瘡と深い褥瘡とに分類して考えるとわかりやすい。感染の合併は殆ど深い褥瘡に限られる。急性期では紅斑、紫斑（つまり皮膚の出血）や水疱、壊死の形になることが多い。この時期では症状の推移をこまめに観察することが必要である。そのためには保護と病変部の観察が可能なポリウレタンフィルム（バイオクルーシブなど）を貼付し数日経過観察し、1－2週程で深さの評価ができる。浅い褥瘡の場合は引き続き、一般医での治療が可能である。深い褥瘡の場合は専門医に紹介したほうがよいことが多い。特に周囲が赤くなり、炎症症状が強い時は早急な対応が必要である。

2）発症原因の推察：

褥瘡の発症には通常基礎疾患の関与があるので、どのような誘因によって褥瘡が発症したのかを十分考える。原疾患の急性期では臥床によって褥瘡が発症するため臥位ポジションによって発症する仙骨部、踵部の褥瘡が多い。回復期ではギャッジアップポジションでの栄養の注入や経口での食事摂取、車椅子座位が開始されるために、尾骨や坐骨の褥瘡が多い傾向がある。腸骨部、大転子部では慢性疾患による麻痺や体の変形によっておこることがしばしばである。

3）原因の除去：

これが最も大切である。適切な体圧分散寝具を用いて因子を除去する。しかし、高齢者の除圧は必ずしも容易ではない。適切に行われているかの判断はドレッシングにずれがないか、創部に新たな出血はないかを観察する。

## 5 専門医紹介のポイント

黒色の大きな壊死組織の存在、周囲が発赤、腫脹、創感染による発熱、膿の排出、大きなポケットの存在である。半年以上治癒しないものも専門医に相談したほうがよい。専門医は外科的デブリドマン、感染症などの合併症の診断と治療、難治性の病態の診断と治療を行う。

逆に専門医から一般医にお願いする場合は感染が沈静化しており、骨や腱などの深部組織の露出がなく、良好な肉芽組織からなる回復期（赤色期）であることが望ましい。大きさは原則として問題ではない。創傷被覆材もしくは外用剤で改善傾向にあることが必要である。その流れを図に示した。

## 6 浅い褥瘡、治癒期の褥瘡の治療

急性期を経過した浅い褥瘡は創傷被覆材もしくは外用剤で治療する。消毒とガーゼの組み合わせでは、創の水分が保てなくて治癒が遷延するので、ウエットドレッシングが提唱されている。デュオアクティブなどのハイドロコロイドやハイドロゲルなどが使いやすい。外用剤ではアクトシン軟膏やリフラップ軟膏を使うことが多い。深い褥瘡では黒色期、黄色期、赤色期、白色期という病期を経過して治癒するが、明らかな軽快傾向にある赤色期、白色期では浅い褥瘡に準じた外用剤や創傷被覆材で一般医が治療可能である（図参照）。詳細は文献2を参考にされたい。

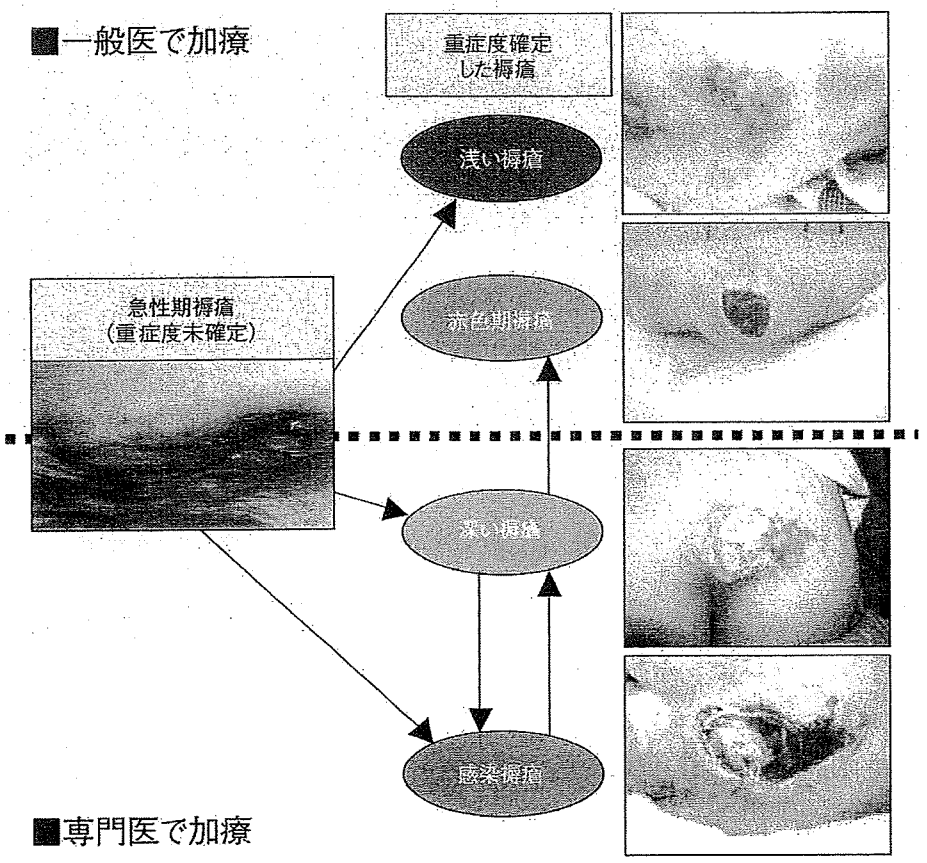


図

（磯貝　善蔵）

## 7 文献

1）日本褥瘡学会編集：褥瘡対策の指針：照林社、東京、2002年、5-26
2）古田勝経：褥瘡外用療法のヒミツ：薬局別冊、南山堂、東京、2006年、25-38

# G2A Plays Proinflammatory Roles in Human Keratinocytes under Oxidative Stress as a Receptor for 9-Hydroxyoctadecadienoic Acid

Tomoyasu Hattori[1,2], Hideru Obinata[1], Ai Ogawa[1,2], Mikiko Kishi[1], Kazuaki Tatei[1], Osamu Ishikawa[2] and Takashi Izumi[1]

G2A is a stress-inducible G protein-coupled receptor for oxidized free fatty acids, such as 9-hydroxyoctadecadienoic acid (HODE). As skin is routinely and pathologically exposed to many oxidative stresses such as UV radiation, chemical agents, and inflammation that might induce both G2A expression and production of G2A ligands, we examined G2A function in human keratinocytes. G2A was expressed in human epidermis, normal human epidermal keratinocytes (NHEK), and an immortalized human keratinocyte cell line (HaCaT). 9(*S*)-HODE evoked intracellular calcium mobilization and secretion of cytokines, including IL-6, IL-8, and GM-CSF in NHEK cells. These responses became prominent in HaCaT cells by overexpression of G2A. 9(*S*)-HODE inhibited proliferation of NHEK cells by suppressing DNA synthesis and arresting the cell cycle in the G0/1-phase. On the other hand, 13(*S*)-HODE, another major oxidative product from linoleate, showed little or no effect on either cytokine secretion or on proliferation in NHEK cells. A small interfering RNA designed to downregulate G2A caused suppression of 9(*S*)-HODE-induced inhibitory effects on proliferation of NHEK cells. UVB and $H_2O_2$ induced G2A expression and caused oxidation of linoleate to produce 9-HODE in HaCaT cells. These results suggest that 9-HODE-G2A signaling plays proinflammatory roles in skin under oxidative conditions.

*Journal of Investigative Dermatology* (2008) **128,** 1123–1133; doi:10.1038/sj.jid.5701172; published online 22 November 2007

## INTRODUCTION

G2A (derived from G2 accumulation) was first identified as a stress-inducible G protein-coupled receptor (GPCR) predominantly expressed in lymphoid tissues and macrophages (Weng *et al.*, 1998). Exogenous expression of G2A is known to cause cell cycle arrest in the G2/M-phase (Weng *et al.*, 1998). Mice lacking G2A develop a late-onset autoimmune syndrome (Le *et al.*, 2001), suggesting that G2A plays a critical role in controlling peripheral lymphocyte homeostasis.

Controversial findings have been reported on endogenous ligands of G2A. At first, lysophosphatidylcholine and sphingosylphosphorylcholine were reported as potent ligands for G2A (Kabarowski *et al.*, 2001). However, the specific binding of lysophosphatidylcholine to G2A-expressing cells has not been reproducible (Witte *et al.*, 2005). Another report showed that G2A was a proton-sensing GPCR (Murakami *et al.*, 2004), along with three other related GPCRs, that is, OGR1, GPR4, and TDAG8. These receptors mediate accumulation of intracellular inositol phosphates or cAMP in response to acidic pH. However, G2A was reported to be less sensitive to pH fluctuations than the other three receptors in immune cells (Radu *et al.*, 2005).

We recently reported another function of G2A as a receptor for oxidized free fatty acids, such as 9-hydroxyoctadecadienoic acid (HODE) and 11-hydroxyeicosatetraenoic acid (Obinata *et al.*, 2005). When G2A was expressed in CHO-K1 or HEK293 cells, 9-HODE induced [$^{35}$S]GTPγS binding, intracellular calcium mobilization, inhibition of cAMP accumulation, and activation of a mitogen-activated protein kinase, JNK. However, the biological significance of G2A still remains unsolved.

While oxidized free fatty acids can be produced by many kinds of oxidative stresses, G2A was identified as a stress-inducible GPCR (Weng *et al.*, 1998). Therefore, oxidative stresses might induce both ligand production and receptor expression to mediate appropriate cellular responses. As skin is routinely or pathologically exposed to many oxidative stresses, oxidized free fatty acid-G2A signaling might play biological roles in various conditions evoked by UV radiation, chemical agents, inflammation, microorganism infection, and other oxidative stresses in skin.

[1]*Department of Molecular Biochemistry, Gunma University Graduate School of Medicine, Maebashi, Gunma, Japan and* [2]*Department of Dermatology, Gunma University Graduate School of Medicine, Maebashi, Gunma, Japan*

*Correspondence: Dr Takashi Izumi, Department of Molecular Biochemistry, Gunma University Graduate School of Medicine, 3-39-22 Showa-machi, Maebashi, Gunma 371-8511, Japan. E-mail: takizumi@med.gunma-u.ac.jp*

*Abbreviations: GPCR, G protein-coupled receptor; HODE, hydroxyoctadecadienoic acid; NHEK, normal human epidermal keratinocyte; PBS, phosphate-buffered saline; PPAR, peroxisome proliferator-activated receptor; ROS, reactive oxygen species; siRNA, small interfering RNA; RT, reverse transcriptase*

*Received 22 January 2007; revised 20 September 2007; accepted 1 October 2007; published online 22 November 2007*

In skin, UV radiation can cause sunburns, skin cancer, skin aging, and immune suppression (Bickers and Athar, 2006). Keratinocytes are damaged mainly by medium-wavelength UV (UVB; 290–320 nm) (Ichihashi *et al.*, 2003). UVB absorption by keratinocytes results in DNA damage and generation of reactive oxygen species (ROS) (Heck *et al.*, 2003; Ichihashi *et al.*, 2003). Epidermis is rich in linoleic acid that exists as a free acid or is incorporated into acylceramide and phospholipid (Marcelo *et al.*, 1992; Vicanova *et al.*, 1999; Terashi *et al.*, 2000). Under the conditions with UVB radiation in skin, lipids containing linoleic acid might be oxidized, resulting in the production of 9-HODE, which acts as a ligand of G2A. In this study, we examined the effects of 9(*S*)-HODE on human keratinocytes, and the involvement of G2A in 9(*S*)-HODE-induced effects. We found that 9(*S*)-HODE evoked intracellular calcium mobilization and secretion of cytokines, which were enhanced by overexpression of G2A. 9(*S*)-HODE inhibited proliferation of keratinocytes due to cell cycle arrest in the G0/1-phase. Furthermore, UV and $H_2O_2$ caused G2A induction and 9-HODE production, and the UV-induced G2A was functional in secretion of cytokines. These results suggest that G2A plays biological roles as a receptor for 9-HODE under oxidative conditions in skin.

## RESULTS

### Expression of G2A in human keratinocytes

First, the expression of G2A was examined in normal human skin by immunohistochemical analysis. Sections from shoulder skin were treated with a specific antibody against the second cytoplasmic domain of human G2A. G2A was expressed in the epidermis preferentially in the spinous and granular cell layers, whereas its expression was lower in the basal cell layer (Figure 1a, upper sides). G2A was preferentially expressed on the cell membrane of normal human epidermal keratinocytes (NHEK) and an immortalized human keratinocyte cell line (HaCaT) (Figure 1a, middle and lower left sides). Competition studies of the G2A antibody with blocking peptide decreased the signals observed in both cells (Figure 1a, middle and lower right sides). G2A protein was detected as a single band of ~42 kDa, compatible with the molecular weight of 42,368 calculated from the amino acid sequence of human G2A, in the membrane fractions of NHEK and HaCaT cells by western blotting, and the pretreatment with blocking peptide to the G2A antibody resulted in elimination of the band (Figure 1b). These data suggested that the antibody used specifically bound to G2A protein. Expression of G2A mRNA in cultured human keratinocytes was also examined. Total RNA was extracted from NHEK and HaCaT cells, and reverse transcriptase (RT)-PCR analysis was performed. G2A mRNA was expressed in both types of keratinocytes (Figure 1c). The level of G2A mRNA in NHEK cells at the fourth passage was estimated to be $10^4$ order copies per μg of total RNA using quantitative real-time RT-PCR (data not shown).

### Intracellular calcium mobilization evoked by 9(*S*)-HODE

Next, we examined whether 9(*S*)-HODE could mediate any intracellular signals in NHEK cells, which endogenously express G2A. The intracellular calcium concentration was significantly increased with 10 μM 9(*S*)-HODE (Figure 2a).

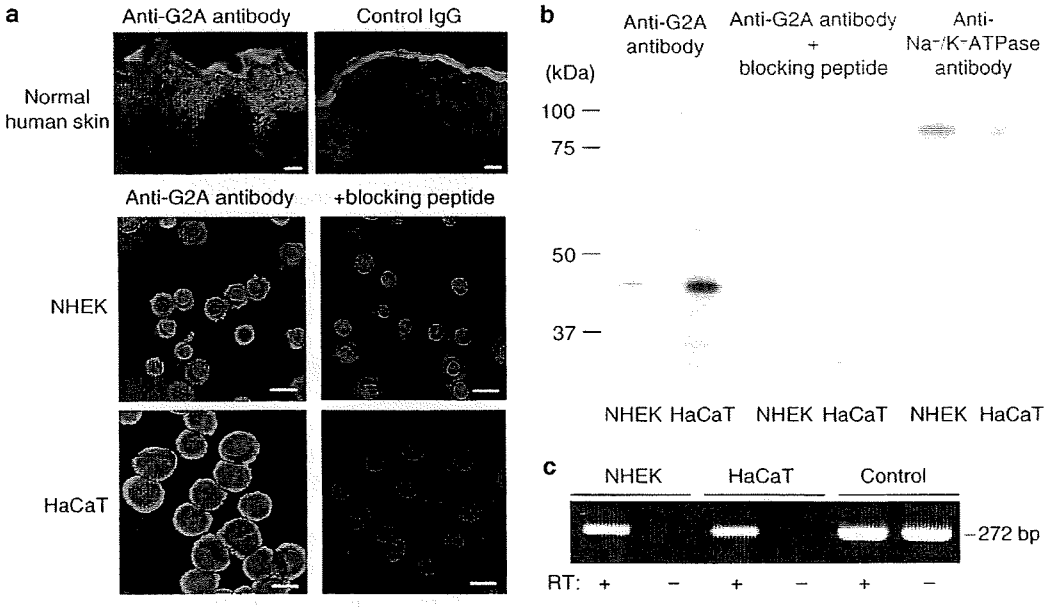


**Figure 1. Expression of G2A in human keratinocytes.** (**a**) Immunostaining for G2A in normal human skin, NHEK, and HaCaT cells. The primary antibody was a specific antibody against G2A or normal control rabbit IgG. The nuclei of NHEK and HaCaT cells were stained with SYTOX Orange Nucleic Acid Stain. For the competition study of G2A antibody, the primary antibody was preabsorbed with G2A blocking peptide. Bar = 20 μm. (**b**) Western blotting of the membrane fractions (0.5 μg per lane) from NHEK and HaCaT cells to detect G2A or $Na^+/K^+$ ATPase. (**c**) Detection of G2A mRNA in cultured human keratinocytes. Expression of G2A mRNA was examined by PCR with or without RT reaction. The pCXN2.1-G2A vector was used as a template for positive controls. Data are representative of three independent experiments.

Sequential application of 15 μM 9(*S*)-HODE did not evoke any further responses, possibly due to receptor desensitization, as the cells could still respond to 10 μM ATP. In dose–response experiments, the calcium increase with 3 μM of 9(*S*)-HODE was significant and the maximal response was observed with 10 μM of 9(*S*)-HODE (Figure 2b).

To confirm the involvement of G2A in 9(*S*)-HODE-induced calcium mobilization, we analyzed calcium responses in HaCaT cells. As parental HaCaT cells did not show any significant responses up to 10 μM 9(*S*)-HODE, a polyclonal population of HaCaT cells that stably overexpress FLAG-tagged G2A (HaCaT-G2A) was established. Cell surface expression of FLAG-tagged G2A proteins was confirmed by flow cytometric analysis using an anti-FLAG antibody (Figure 2c). Stable expression of G2A in HaCaT cells caused a significant calcium response with 9(*S*)-HODE (Figure 2d). 9(*S*)-HODE at 10 μM evoked an increase in the intracellular calcium concentration by 51.6 ± 5.25 nM (Figure 2e, mean ± SD; $n = 4$). The response to 13(*S*)-HODE, less active ligand for G2A (Obinata *et al.*, 2005), was less than half of that to 9(*S*)-HODE in HaCaT-G2A cells (Figure 2e). These results indicate that 9(*S*)-HODE induced intracellular calcium mobilization through G2A in NHEK and HaCaT cells.

### Cytokine secretion evoked by 9(*S*)-HODE in NHEK cells

Keratinocytes have been reported to produce various cytokines, including IL-1, -6, -8, -10, -12, GM-CSF, tumor necrosis factor-α, and so on, in response to diverse stimuli (McKenzie and Sauder, 1990; Grone, 2002). We examined whether 9(*S*)-HODE induced cytokine secretion in NHEK cells. Among various cytokines examined, 9(*S*)-HODE induced productions of IL-6 (Figure 3a), IL-8 (Figure 3b), and GM-CSF (Figure 3c) in

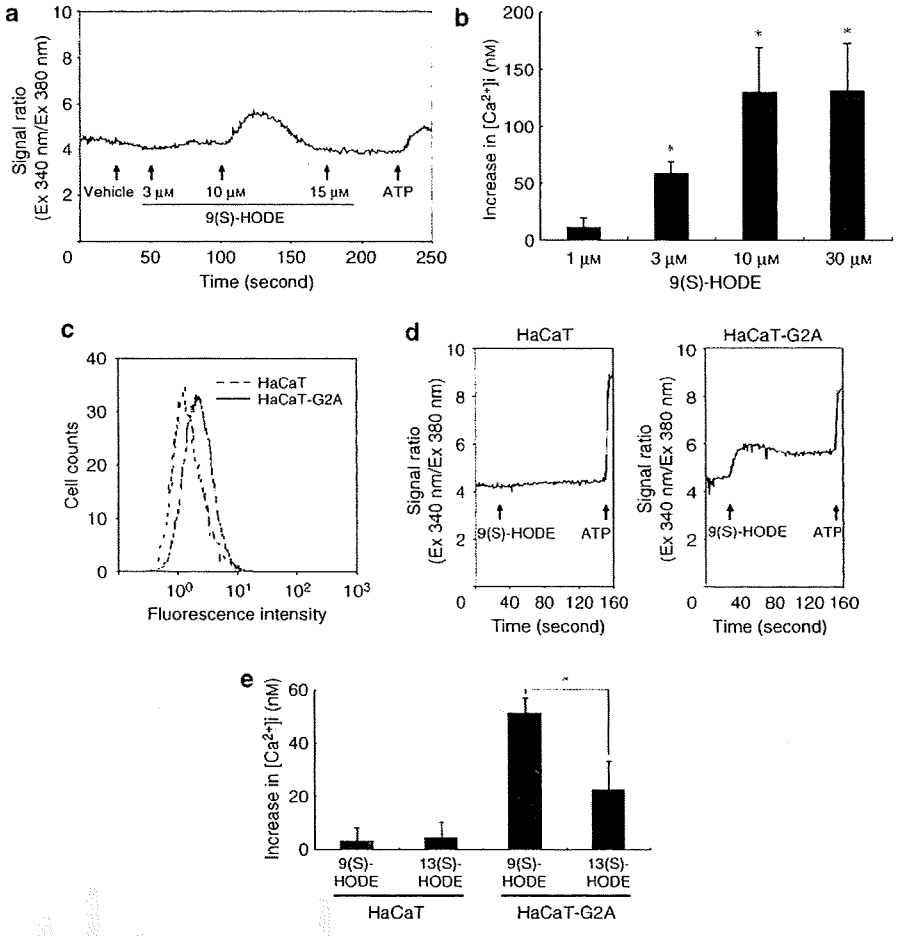


**Figure 2. Intracellular calcium mobilization via G2A evoked by 9(*S*)-HODE.** (**a**) Intracellular calcium mobilization in NHEK cells measured by an RF5300PC spectrofluorometer. Cells loaded with Fura-2/AM were stimulated with increasing concentrations of 9(*S*)-HODE. As a positive control, cells were stimulated with 10 μM ATP. (**b**) Calcium responses with various concentrations of 9(*S*)-HODE in NHEK cells ($n = 4$, $^*P < 0.01$ (Student's *t*-test) vs corresponding values of 1 μM). Before stimulation, 9(*S*)-HODE was dissolved in HEPES-Tyrode's-BSA buffer after evaporation of ethanol under nitrogen gas. (**c**) Cell surface expression of exogenous G2A. Stable transformants of HaCaT cells that overexpress FLAG-tagged G2A were established (HaCaT-G2A). FLAG-tagged G2A was detected by flow cytometry using an M5 anti-FLAG antibody. Dotted line, HaCaT cells; solid line, HaCaT-G2A cells. (**d**) Intracellular calcium mobilization in HaCaT and HaCaT-G2A cells. Cells were stimulated with 10 μM 9(*S*)-HODE and 10 μM ATP. (**e**) Quantification of changes in intracellular calcium concentrations after stimulation with HODEs at the concentration of 10 μM. Data represent mean + SD ($n = 4$, $^*P < 0.01$ (Student's *t*-test)). Data are representative of three independent experiments. Ex, excitation.

dose-dependent manners. Elevation of cytokine levels became evident at 4 hours in IL-6 and IL-8, and 16 hours in GM-CSF after 9(*S*)-HODE treatment. As shown in Figure 3d and e, 10 μM 13(*S*)-HODE did not induce productions of IL-6 and IL-8 8 hours after the treatment. These data indicate that 9(*S*)-HODE induces cytokine secretion in NHEK cells via G2A but not through such mechanisms as toxic effects of oxidized free fatty acids.

**Involvement of G2A in cytokine secretion evoked by 9(*S*)-HODE in HaCaT cells**

To examine the involvement of G2A in 9(*S*)-HODE-induced cytokine secretion, we analyzed 9(*S*)-HODE-induced IL-6 and IL-8 secretion in HaCaT-G2A cells. While HODEs did not induce cytokine secretion in parental HaCaT cells, overexpression of G2A in HaCaT cells resulted in significant increases in IL-6 and IL-8 releases 8 hours after 9(*S*)-HODE treatment (Figure S1, right sides, filled squares). The amounts of both cytokines induced by 13(*S*)-HODE were much smaller than those induced by 9(*S*)-HODE in HaCaT-G2A cells (Figure S1, right sides, striped squares). Without HODEs treatment, both cytokine levels in the culture supernatant of HaCaT-G2A cells were higher than those of HaCaT cells (Figure S1, open squares), possibly due to the constitutive activity of G2A as shown in HeLa cells exogenously expressing G2A (Lin and Ye, 2003). Taken together with the results in NHEK cells (Figure 3), these results indicate that cytokine secretion evoked by 9(*S*)-HODE was mediated via G2A in keratinocytes.

**Inhibition of proliferation and morphological changes by 9(*S*)-HODE in NHEK cells**

Next, we examined whether 9(*S*)-HODE had any effects on the proliferation of keratinocytes. Cell viability was determined by measuring the contents of ATP in the cells. Cell viability was decreased by 9(*S*)-HODE treatment in a dose-dependent manner (Figure 4a). The treatment with 10 μM 9(*S*)-HODE strongly decreased cell viability, and this effect continued for 48 hours accompanied by morphological changes in NHEK cells (Figure 4b). The light microscopic images, taken 24 hours after 9(*S*)-HODE treatment, showed that 9(*S*)-HODE-treated cells contained enlarged cytoplasm and distinct shiny perinuclear vesicles with a diameter of approximately 1 μm. The cytoplasm swelling was more apparent 48 hours after 9(*S*)-HODE treatment, and elongated cells appeared with the shiny granules located on top of keratinocyte colonies. On the other hand, the treatment with 10 μM 13(*S*)-HODE did not affect the cell viability (Figure 4c) and neither did it change the morphology of NHEK cells (data not shown). To examine the involvement of G2A in 9(*S*)-HODE-induced decrease of cell viability in NHEK cells, we tried to suppress the expression of G2A using small interfering RNA (siRNA). An siRNA, named siRNA-132, decreased the expression of G2A mRNA to 61% of that of scrambled control cells in a quantitative real-time RT-PCR analysis (Figure 4d). By this siRNA-mediated suppression of G2A, the decrease of the cell viability 24 hours after 9(*S*)-HODE treatment was partially inhibited (Figure 4e). These data indicate that 9(*S*)-HODE induced suppression of proliferation via G2A in NHEK cells. On the other hand, cell viability was not significantly affected in both HaCaT and HaCaT-G2A cells by the treatment with 10 μM 9(*S*)-HODE (discussed later).

**Suppression of DNA synthesis and cell cycle arrest in the G0/1-phase by 9(*S*)-HODE in NHEK cells**

To elucidate the mechanisms of 9(*S*)-HODE-induced inhibition of the proliferation in NHEK cells, cell cycle analysis was performed. NHEK cells were treated with 10 μM 9(*S*)-HODE for 24 hours and stained with propidium iodide, followed by flow cytometric analysis of the cell cycle distribution. 9(*S*)-HODE increased the cell percentage in the G0/1-phase by 20% and decreased the cell percentage in the S-phase by

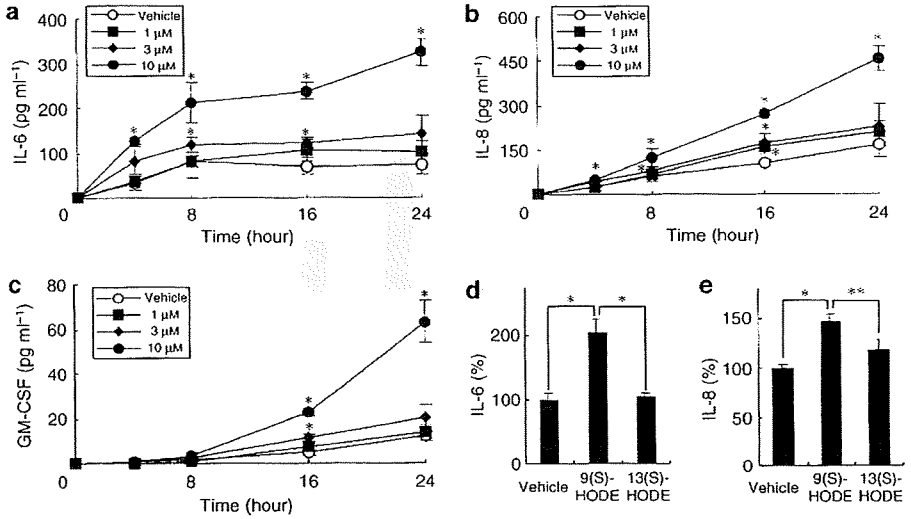


**Figure 3. Cytokine secretion evoked by 9(*S*)-HODE in NHEK cells.** (a–c) Cytokine productions evoked by various concentrations of 9(*S*)-HODE. (**a**) IL-6; (**b**) IL-8; (**c**) GM-CSF. ($n=3$, $^*P<0.05$ (Student's *t*-test) vs corresponding values of vehicle control). (**d**, **e**) Cytokine productions evoked by HODEs at the concentration of 10 μM 8 hours after the treatment. (**d**) IL-6; (**e**) IL-8 ($^*P<0.01$, $^{**}P<0.05$ (Student's *t*-test)). Data are representative of three independent experiments.

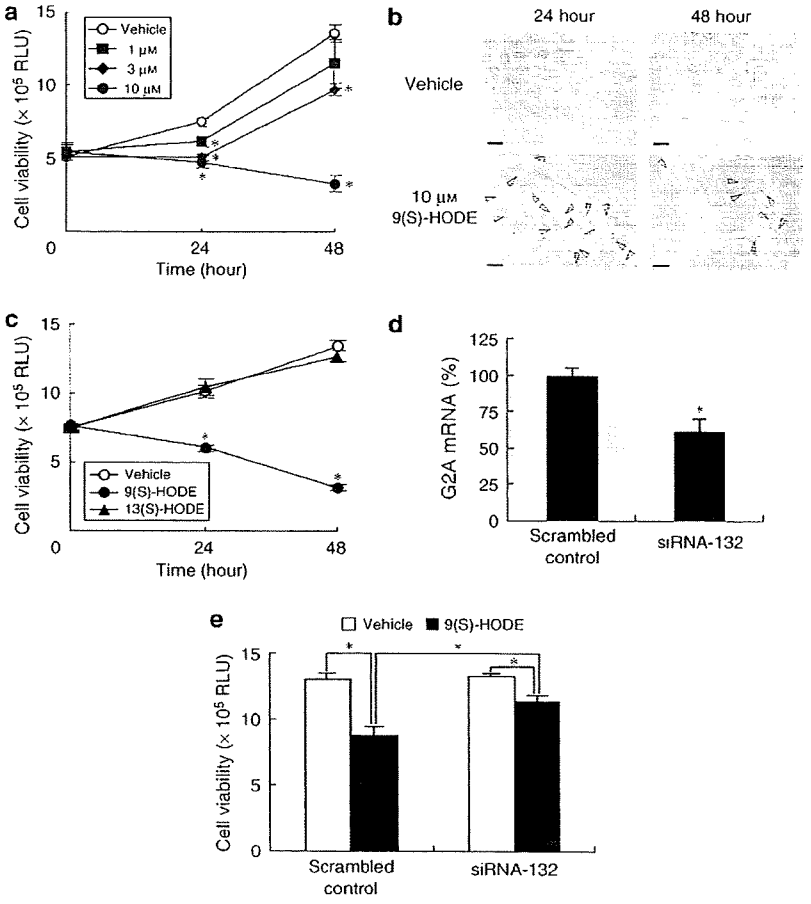


**Figure 4. Inhibition of proliferation by 9(*S*)-HODE in NHEK cells.** (a) Cell viability of NHEK cells treated with various concentrations of 9(*S*)-HODE in the growth medium ($n=4$, $^*P<0.01$ (Student's *t*-test) vs corresponding values of vehicle control). RLU, relative luminescence units. (b) Morphology of cells treated with 10 μM 9(*S*)-HODE. The open arrowheads show typical shiny perinuclear vesicles. Original magnification is 400-fold. Bar = 20 μm. (c) Cell viability of NHEK cells treated with HODEs at the concentration of 10 μM ($n=4$, $^*P<0.01$ (Student's *t*-test) vs corresponding values of vehicle control). (d) Effects of siRNA-132 on the expression of G2A mRNA in NHEK cells 48 hours after transfection of siRNAs ($n=3$, $^*P<0.01$ (Student's *t*-test) vs corresponding values of scrambled control). (e) siRNA-mediated inhibition of 9(*S*)-HODE-induced effects on cell viability of NHEK cells 24 hours after 10 μM 9(*S*)-HODE treatment ($n=3$, $^*P<0.01$ (Student's *t*-test)). Data are representative of three independent experiments.

more than 10% (Figure S2a and b). The cell percentage of sub-G1 cells, apoptotic cells with degraded DNA, was not changed by 9(*S*)-HODE treatment, while it increased after 10 mJ cm$^{-2}$ UVB irradiation. DNA fragmentation was not detected in cells treated with 10 μM 9(*S*)-HODE, while it was obvious in the cells irradiated with UVB (Figure S2c). To examine the effects of 9(*S*)-HODE on DNA synthesis in NHEK cells, incorporation of BrdU, an analogue of thymidine, was measured. Treatment with 10 μM 9(*S*)-HODE decreased BrdU incorporation to 40% of that of vehicle control in NHEK cells (Figure S2d). These results suggested that 9(*S*)-HODE inhibited proliferation of NHEK cells, which was caused by suppression of DNA synthesis and cell cycle arrest in the G0/1-phase, but not by apoptosis.

### Induction of G2A by UVB and $H_2O_2$

Since G2A was reported as a DNA damage- and stress-inducible GPCR (Weng *et al.*, 1998), we examined levels of G2A mRNA in cultured keratinocytes irradiated with various doses of UVB. UVB increased G2A mRNA in a dose-dependent manner in HaCaT cells 24 hours after irradiation up to 10 mJ cm$^{-2}$. The level of G2A mRNA in 10 mJ cm$^{-2}$ UVB-irradiated cells was nearly double than that in mock-irradiated cells (Figure 5a). Hydrogen peroxide ($H_2O_2$) treatment at 100 μM also increased G2A mRNA in HaCaT cells (Figure 5b). The levels of glyceraldehyde-3-phosphate dehydrogenase mRNA were simultaneously analyzed, but they did not change in HaCaT cells under these experimental conditions (data not shown). Next, ROS productions were analyzed using CM-$H_2$DCFDA dye, which was oxidized by ROS to the highly fluorescent 2′,7′-dichlorofluorescein. The fluorescence intensity was increased by both UVB and $H_2O_2$ in HaCaT cells (Figure 5c). The increase became significant immediately after UVB irradiation and 30 minutes after $H_2O_2$ treatment, respectively. Thus, the induction of G2A by these two stimuli was accompanied by ROS production.

Next, we examined whether UVB-induced G2A enhanced cytokine secretion evoked by 9(*S*)-HODE. HaCaT cells were

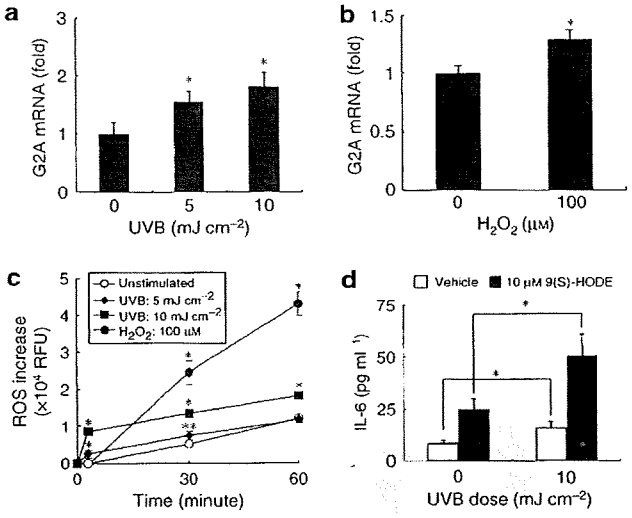


**Figure 5. Induction of G2A by UVB and $H_2O_2$.** (**a**, **b**) Expression levels of G2A mRNA in HaCaT cells 24 hours after (**a**) UVB irradiation or (**b**) $H_2O_2$ treatment. A quantitative real-time RT-PCR analysis was performed ($n=4$, $^*P<0.01$ (Student's *t*-test) vs corresponding values of (**a**) mock-irradiated cells, and (**b**) unstimulated control). (**c**) Detection of ROS production after UVB irradiation or $H_2O_2$ treatment in HaCaT cells ($n=4$, $^*P<0.01$, $^{**}P<0.05$ (Student's *t*-test) vs corresponding values of unstimulated control). RFU, relative fluorescence units. (**d**) Increase of 9(*S*)-HODE-induced IL-6 production after UVB irradiation in HaCaT cells. HaCaT cells were irradiated (10 mJ cm$^{-2}$ UVB) or mock-irradiated in PBS and cultured in DMEM containing 10% fetal bovine serum. After 12 hours, cells were serum-starved and cultured for another 12 hours. The cells were then treated with 10 μM 9(*S*)-HODE in DMEM, and concentrations of IL-6 at 8 hours were measured using a Bio-Plex ELISA system ($n=3$, $^*P<0.05$ (Student's *t*-test)). Data are representative of three independent experiments.

irradiated with 10 mJ cm$^{-2}$ UVB, incubated for 24 hours, and treated with 10 μM 9(*S*)-HODE. As shown in Figure 5d, the level of IL-6 8 hours after 9(*S*)-HODE treatment was significantly higher in UVB-irradiated cells than in mock-irradiated cells (see filled squares). Without 9(*S*)-HODE treatment, IL-6 production was increased in UVB-irradiated cells (see open squares) probably due to the constitutive activity of the induced G2A as shown in Figure S1. These data indicate that functional G2A was induced by UVB irradiation in keratinocytes.

### Production of 9-HODE by UVB and $H_2O_2$

Finally, we examined whether oxidative stresses cause conversion of linoleic acid to 9-HODE. Among the derivatives of linoleic acid, 9-HODE and 9-hydroperoxyoctadecadienoic acid were the most potent ligands of G2A, while 13-HODE and 13-hydroperoxyoctadecadienoic acid were much less active (Obinata *et al.*, 2005). We quantified the amounts of HODEs (9-(*E*,*Z*)-HODE and 13-(*Z*,*E*)-HODE) in UVB-irradiated linoleic acid by liquid chromatography-mass spectrometry using deuterated-9-HODE as an internal standard after chemical reduction of hydroperoxyoctadecadienoic acids to HODEs (Supplementary Materials and Methods). As shown in Figure S3, 100 mJ cm$^{-2}$ UVB increased the level of 9-HODE. At the same time, 13-HODE was produced at comparable level to 9-HODE. The increase became prominent 2 minutes after the irradiation (9-HODE, about 4.1 ng per dish; Figure S3a) and reached a plateau after 10 minutes (9-HODE, about 6.0 ng per dish; Figure S3a). The production of HODEs was dependent on the dose of UVB (Figure S3b). The dose required for the significant increase of 9-HODE was 25 mJ cm$^{-2}$, but 10 mJ cm$^{-2}$ UVB had a tendency to produce 9-HODE. These results suggest that G2A ligands are produced from polyunsaturated fatty acids, such as linoleic acid, possibly through radical reaction, when they are directly exposed to UVB. Furthermore, we examined whether UVB caused 9-HODE production in HaCaT cells. As cultured keratinocytes are thought to be in an essential fatty acid-deficient state (Marcelo *et al.*, 1992; Vicanova *et al.*, 1999), we supplemented HaCaT cells with linoleic acid before UVB irradiation to observe linoleate oxidation sensitively. Total lipids extracted from stimulated cells were analyzed by liquid chromatography-mass spectrometry after treatment with phospholipase $A_2$ and chemical reduction. As shown in Figure S3c, the levels of 9-HODE and 13-HODE were increased approximately twofold 30 minutes after UVB irradiation (100 mJ cm$^{-2}$). Treatment with 200 μM $H_2O_2$ also resulted in increased oxidation of linoleate (approximately threefold; Figure S3c). The increase was not observed without phospholipase $A_2$ treatment (data not shown), suggesting that linoleate was oxidized in its esterified form in phospholipids. These data indicate that keratinocytes might produce G2A ligands under oxidative stresses.

## DISCUSSION

G2A was first identified as a GPCR that could be induced by various DNA-damaging and stress-inducing stimuli, including UV irradiation in human Ramos B cells (Weng *et al.*, 1998). In this study, we showed that G2A was also expressed in human epidermis and keratinocytes (Figure 1), and the expression was increased by UVB and $H_2O_2$ (Figure 5). We further showed that these oxidative stimuli caused 9-HODE production (Figure S3). 9(*S*)-HODE induced intracellular calcium mobilization (Figure 2), cytokine production (Figure 3), and inhibition of proliferation (Figure 4) in keratinocytes, while 13(*S*)-HODE revealed no effect or much smaller effects than 9(*S*)-HODE (Figures 2e, 3d, e, and 4c, and Figure S1). These responses were enhanced by overexpression or induction of G2A (Figures 2d, e, and 5d, and Figure S1) and were attenuated by decrease of G2A (Figure 4e). Thus, we conclude that these 9(*S*)-HODE-induced responses are mediated via G2A and assume that G2A plays biological roles in skin as a receptor for 9-HODE.

There were some differences in response to 9-HODE between NHEK and HaCaT cells. Although HaCaT cells seemed to possess more G2A protein than NHEK cells (Figure 1b), HaCaT cells showed much smaller responses to 9-HODE than NHEK cells in cytokine production (Figure S1) and no response in calcium mobilization (Figure 2d). HaCaT cells came to show significant responses to 9-HODE after expressing exogenous G2A in HaCaT-G2A cells (Figure 2e and Figure S1). The reason why parent HaCaT cells did not show apparent response to 9-HODE remains to be elucidated.

Some oxidative derivatives of linoleic and arachidonic acids can activate G2A. Among them, free 9-HODE is the most potent in mediating intracellular calcium mobilization in CHO-K1 cells expressing G2A (Obinata *et al.*, 2005). 9-HODE can be produced by oxidation of linoleic acid through both radical and enzymatic reactions, and linoleic acid is the most commonly found polyunsaturated fatty acid in epidermis (Marcelo *et al.*, 1992; Vicanova *et al.*, 1999). Oxidative stresses, such as UV radiation, gaseous pollutants, chemical agents, microorganism infection, skin cancer, and inflammations, are supposed to induce radical reactions in skin and lead to induction of cutaneous lipid peroxidation with concomitant modulation in the level of antioxidant and drug-metabolizing enzymes (Bickers and Athar, 2006). For instance, free radical oxidation was reported as the main process in producing oxidized derivatives of linoleic acid, including 9-HODE in mouse skin treated with phorbol myristate acetate (Beckman *et al.*, 1994). Furthermore, enzymatic reaction of prostaglandin H-synthase-2 has been found to convert linoleic acid to 9-HODE in mouse keratinocytes and human dermal fibroblasts under stimulation of epidermal growth factor (Loftin and Eling, 1996) and IL-1β (Godessart *et al.*, 1996), respectively. Some of the lipoxygenases and cytochrome P450 enzymes would also be involved in the metabolism of linoleic and arachidonic acids in skin.

Linoleic acid is known to be essential for proper cutaneous barrier function, and linoleic acid-rich acylceramide is believed to have a specific function in the formation of stratum corneum lipid layers (Wright, 1991). In addition to ceramides, cholesterol and free fatty acids are rich in the stratum corneum, and linoleic acid is the most abundant polyunsaturated fatty acid in free fatty acid fractions (Vicanova *et al.*, 1999). In this context, when skin is exposed to oxidative stresses, free linoleic acid might be converted to free 9-HODE in the uppermost layer of the epidermis as shown in Figure S3a and b. Also, linoleic acid-containing acylceramide and cholesterol ester in the stratum corneum could be oxidized and then hydrolyzed to produce free 9-HODE.

In epidermal cell layers, linoleic acid exists abundantly as linoleate esterified to phospholipids of cell membranes in the suprabasal and basal cell layers (Marcelo *et al.*, 1992; Terashi *et al.*, 2000). In normal human skin, 9-HODE esterified to phospholipids was identified by biochemical analyses (Gron *et al.*, 1993a). In this study, the oxidation of linoleate in the membrane lipid of HaCaT cells by UVB and $H_2O_2$ was observed after the *in vitro* treatment with phospholipase $A_2$ (Figure S3c). In skin under oxidative conditions, oxidized linoleate could be hydrolyzed to produce HODEs by phospholipase $A_2$ that might be activated by ROS signaling pathway. In psoriatic skin, 9-HODE has been detected as a free acid (Baer *et al.*, 1990; Baer *et al.*, 1991; Gron *et al.*, 1993b; Bayer *et al.*, 2005), and levels of 9-HODE esterified to the *sn*-2 position of phospholipids in lesional psoriatic skin are significantly decreased compared with non-lesional psoriatic skin (Gron *et al.*, 1993b). It is possible that membrane phospholipids are hydrolyzed by certain types of phospholipase $A_2$ generating free 9-HODE in lesional psoriatic skin. An epithelium-specific cytosolic phospholipase $A_2$ (cytosolic $PLA_2\delta$) was reported to be induced in psoriatic skin (Chiba *et al.*, 2004).

Many of the UVB-induced damages in keratinocytes might be mediated by ROS and subsequently induced cytokines. Production of ROS causes oxidation of lipids. In this report, UVB was found to cause both production of 9-HODE (Figure S3) and induction of G2A expression (Figure 5a) accompanied by ROS production (Figure 5c) in keratinocytes. Cytokine secretion evoked by 9(*S*)-HODE was enhanced in cells irradiated with UVB (Figure 5d). Intensity of UVB ($5\ mJ\ cm^{-2}$) required for G2A induction is lower than those used in previous reports in which effects of UVB irradiation on keratinocytes were analyzed (Walterscheid *et al.*, 2002; Marathe *et al.*, 2005). Although higher doses of UVB ($25\ mJ\ cm^{-2}$) were required for the significant increase of 9-HODE converted from linoleic acid, the doses are still in the range we are commonly exposed to in daily life (Caricchio *et al.*, 2003). In case of sunburn, UV irradiation first occurs in stratum corneum that contains linoleic acid-rich lipid layers as discussed above. Then, diminished UV may still have some biological effects in keratinocytes in the granular and spinous cell layers where G2A mainly exists (Figure 1a).

Keratinocytes participate in immune systems by producing various cytokines in response to diverse stimuli. Cytokines released from keratinocytes affect Langerhans cells, lymphocytes, vascular endothelial cells, and keratinocytes themselves to regulate immune responses and inflammatory reactions (McKenzie and Sauder, 1990). In this study, productions of IL-6 and IL-8 were observed in keratinocytes treated with 9(*S*)-HODE (Figure 3a and b), and the levels of IL-6 and IL-8 were increased by overexpression of G2A (Figure S1). IL-6 induces keratinocyte proliferation *in vitro* (Grossman *et al.*, 1989; Yoshizaki *et al.*, 1990). On the other hand, IL-8 is a chemokine, which recruits neutrophils, macrophages, and T cells, whereas IL-8 also promotes keratinocyte proliferation (Tuschil *et al.*, 1992). The abnormally high levels of these cytokines (Grossman *et al.*, 1989; Schroder *et al.*, 1992; Kulke *et al.*, 1996), and the expression pattern of both receptors in psoriasis (Ohta *et al.*, 1991; Kulke *et al.*, 1998) would be associated with the hyperproliferation of keratinocytes and accumulation of neutrophils, which are characteristic findings of psoriatic lesions. In addition to IL-6 and IL-8, GM-CSF was released from keratinocytes by 9(*S*)-HODE stimulation (Figure 3c). 9-HODE was reported to be a strong proinflammatory mediator in an experimental wound-healing model of the rat (Moch *et al.*, 1990). G2A might be involved in the initiation or progression of various pathological conditions, including psoriasis, lichen planus, and pustulosis through cytokine secretion from keratinocytes, affecting keratinocytes and inflammatory cells.

9(*S*)-HODE inhibited proliferation of keratinocytes, which was caused by suppression of DNA synthesis and cell cycle arrest in the G0/1-phase (Figure 4 and Figure S2). G2A overexpression was reported to cause cell accumulation at the G2/M-phase in NIH3T3 cells, although the possibility that G2A might be functional at other checkpoints in the cell cycle was not excluded (Weng *et al.*, 1998). It is reasonable to assume that cell cycle arrest is induced under cell-damaging

conditions such as oxidative stresses. In this study, 9(*S*)-HODE did not inhibit proliferation of HaCaT cells (data not shown). We suppose that HaCaT cells might not be suitable to examine the effects of 9-HODE on cell proliferation because the *p53* mutations, which largely affect the signals of cell cycle, were identified in HaCaT cells (Lehman *et al.*, 1993).

Since 9(*S*)-HODE has been described as one of the endogenous activators of peroxisome proliferator-activated receptor (PPAR)γ (Nagy *et al.*, 1998), it was inferred that some of the effects induced by 9(*S*)-HODE in NHEK cells were mediated via PPARγ. Involvement of PPARγ has been implicated in the regulation of inflammatory processes and cytokine release in various cell types. To examine this possibility, NHEK cells were treated with PPARγ antagonist, GW9662, and assessed using a cell viability assay and a cytokine assay. GW9662 (10 μM) did not inhibit the effects induced by 10 μM 9(*S*)-HODE (data not shown). In a previous study, the required concentration of 9(*S*)-HODE to induce reporter activities of PPARγ was higher than 10 μM in macrophages (Nagy *et al.*, 1998). In contrast, 1 μM 9(*S*)-HODE was effective for production of cytokines (Figure 3) and for inhibition of cell proliferation (Figure 4a) in keratinocytes. Furthermore, the expression of PPARγ is low in undifferentiated keratinocytes, although it is increased during differentiation (Rivier *et al.*, 1998; Westergaard *et al.*, 2001). Taken together, we conclude that the effects of 9(*S*)-HODE observed in this study were mediated via G2A, although it is still possible that PPARγ might have additive, synergistic, or modifying effects during differentiation.

In summary, we showed that G2A was expressed in keratinocytes and was induced by UVB and $H_2O_2$. These oxidative stimuli also caused oxidation of linoleate. G2A was involved in 9(*S*)-HODE-induced intracellular calcium mobilization, secretion of inflammatory cytokines, and inhibition of cell proliferation in keratinocytes. G2A may play proinflammatory roles as a receptor for oxidized free fatty acids such as 9-HODE under oxidative pathological conditions in skin.

## MATERIALS AND METHODS

### Materials

Linoleic acid was purchased from Sigma (St Louis, MO). 9(*S*)-HODE was synthesized from linoleic acid by an enzymatic reaction with potato 5-lipoxygenase as described previously (Obinata *et al.*, 2005). 13(*S*)-HODE was purchased from Cayman Chemical (Ann Arbor, MI). Ethanol (0.1%) was used as a vehicle for HODEs. An expression vector (pCXN2.1-G2A) for FLAG-tagged human G2A (NCBI accession number AF083955) was constructed as described previously (Obinata *et al.*, 2005).

### Immunohistochemistry

Normal human skin tissues were obtained from surgically excised skin with written informed consent. The study was performed in accordance with institutional guidelines set forth by Gunma University School of Medicine and adhered to the Declaration of Helsinki Principles for use of human tissue. Frozen sections (6-μm thick) were blocked in 10% BSA at room temperature for 30 minutes and then incubated with primary antibodies at 4°C overnight. Primary antibodies (1.7 μg ml$^{-1}$) were either rabbit anti-human G2A antibody (MBL, Woburn, MA) or normal rabbit IgG (Santa Cruz Biotechnology, San Diego, CA) for the negative control sections. Following incubation with 2 μg ml$^{-1}$ secondary antibody (goat anti-rabbit IgG conjugated with Alexa Fluor 488; Molecular Probes, Eugene, OR) at room temperature for 1 hour, fluorescence images were collected using a microscope (Axioskop; Carl Zeiss, Oberkochen, Germany). In case of cell staining, suspended NHEK and HaCaT cells were attached to the slide glasses by centrifugation (300 r.p.m., 2 minutes), fixed with 100% methanol, permeabilized with 0.1% Triton X100 for 30 minutes, and blocked in 1% BSA. The cells were then incubated with primary antibody (1.7 μg ml$^{-1}$) at room temperature for 30 minutes. For the competition study of the G2A antibody, cells were stained with the primary antibody preincubated with 10-fold molar volume of G2A blocking peptide (MBL) at room temperature for 60 minutes. Following incubation with 0.67 μg ml$^{-1}$ secondary antibody and 1 μM SYTOX Orange Nucleic Acid Stain (Molecular Probes) at room temperature for 30 minutes, fluorescence images were collected using a confocal microscope (LSM510; Carl Zeiss). Antibodies were diluted in phosphate-buffered saline (PBS) containing 1% BSA.

### Western blotting

NHEK cells were disrupted by sonication in a homogenizing buffer (20 mM Tris-HCl, pH 7.4, 0.25 M sucrose, 10 mM $MgCl_2$, 2 mM EDTA, and Complete protease inhibitor mixture (Roche Applied Science, Indianapolis, IN)). The homogenates were centrifuged for 10 minutes at 800 × *g*, and the resulting supernatants were further centrifuged for 60 minutes at 100,000 × *g*. The precipitates (membrane fractions) were dissolved in the homogenizing buffer containing 0.5% dodecylmaltoside (Dojindo, Kumamoto, Japan). An aliquot of protein (0.5 μg per lane) was separated on 10% SDS-polyacrylamide gel electrophoresis, transferred to a Hybond-P polyvinylidene difluoride membrane (GE Healthcare, Buckinghamshire, UK), blocked in Tris-buffered saline containing 50% Block Ace (Dainippon Sumitomo Pharma, Osaka, Japan) at 4°C overnight, and then incubated with the rabbit anti-human G2A antibody (0.5 μg ml$^{-1}$) or a 500-fold diluted mouse ascites M7-PB-E9, including anti-$Na^+/K^+$-ATPase monoclonal antibody (Sigma) for 1 hour at room temperature. For the competition study of the G2A antibody, the primary antibody was preincubated with 100-fold molar volume of G2A blocking peptide. After incubation with each horseradish peroxidase-conjugated secondary antibody (80 ng ml$^{-1}$) (Santa Cruz Biotechnology), the signals were visualized using an ECL plus Western blotting Detection System (GE Healthcare).

### Cell culture

NHEK from newborn foreskin were obtained from Kurabo (Osaka, Japan) and were maintained in HuMedia-KB2 (Kurabo, basal medium), supplemented with 10 μg ml$^{-1}$ insulin, 0.1 ng ml$^{-1}$ human epidermal growth factor, 0.5 μg ml$^{-1}$ hydrocortisone, 50 μg ml$^{-1}$ gentamicin, 50 ng ml$^{-1}$ amphotericin B, and 0.4% bovine pituitary extract (growth medium). Usually, NHEK cells between third and fifth passages were used for experiments. Immortalized human keratinocyte cell line HaCaT (Boukamp *et al.*, 1988) was maintained in DMEM (Sigma) containing 10% fetal bovine serum. Cells were cultured at 37°C in a humidified incubator with 5% $CO_2$.

### Transfection and stable expression of G2A

HaCaT cells were transfected with pCXN2.1-G2A using Lipofectamine 2000 reagent (Invitrogen, Carlsbad, CA) according to the manufacturer's instructions. Stably transfected clones resistant to 1 mg ml$^{-1}$ Geneticin (Invitrogen) were collected, and expression levels of G2A were confirmed by RT-PCR and flow cytometric analyses. To observe expression of FLAG-tagged G2A proteins on cell surfaces, cells were incubated with 10 μg ml$^{-1}$ M5 anti-FLAG antibody (Sigma) without cell permeabilization, followed by staining with 10 μg ml$^{-1}$ goat anti-mouse IgG conjugated with Alexa Fluor 488 (Molecular Probes), and were analyzed using an EPICS XL flow cytometer system (Beckman Coulter, Fullerton, CA). Cells were treated with each antibody in PBS containing 1% BSA at room temperature for 1 hour.

### RT-PCR analysis

Total RNA was extracted from NHEK or HaCaT cells using an RNeasy Mini kit (Qiagen, Hilden, Germany) with on-column DNase digestion. RT-PCR analysis of G2A mRNA was performed using a QIAquick one step RT-PCR kit (Qiagen) with the following primer set: sense primer, 5′-GGCTTTGCCATCCCTCTC-3′; antisense primer, 5′-GACAGGCACAGAAACACC-3′. Quantitative real-time RT-PCR analysis was performed using a DNA Engine Opticon 2 system (MJ Research, Waltham, MA).

### Measurement of intracellular calcium concentration

NHEK cells were loaded with 2.5 μM Fura-2/AM (Dojindo) in Hepes-Tyrode's-BSA buffer (25 mM Hepes-NaOH, pH 7.4, 140 mM NaCl, 2.7 mM KCl, 1.0 mM $CaCl_2$, 12 mM $NaHCO_3$, 5.6 mM D-glucose, 0.37 mM $NaH_2PO_4$, 0.49 mM $MgCl_2$, and 0.01% fatty acid-free BSA) containing 0.02% pluronic F127 for 1 hour at 37°C. In case of HaCaT cells, the concentrations of Fura-2/AM and F127 were 5 μM and 0.04%, respectively. Cells were washed with Hepes-Tyrode's-BSA buffer, and changes in intracellular calcium concentrations upon ligand stimulation were monitored with an RF5300PC spectrofluorometer (Shimadu, Kyoto, Japan).

### Determination of cytokine concentrations

NHEK and HaCaT cells were treated with HODEs in the basal medium and DMEM, respectively. HaCaT cells were serum-starved before 9(*S*)-HODE treatment. The culture supernatants were collected at indicated times after HODEs treatment, and concentrations of cytokines were measured using a Bio-Plex ELISA system (BioRad, Hercules, CA).

### Viability and morphology of NHEK cells

NHEK cells were treated with various concentrations of HODEs in the growth medium. Cell viability was determined by luminescent signals proportional to amount of ATP in the cells at indicated times using a CellTiter-Glo Luminescent Cell Viability Assay kit (Promega, Madison, WI), according to the manufacturer's instructions. Cell morphology was observed using a microscope (CKX41; Olympus, Tokyo, Japan).

### Suppression of G2A by siRNA

NHEK cells were transfected with siRNAs (Samchully Pharm, Seoul, Korea) using Lipofectamine 2000 reagent. The sequences of G2A-specific (named siRNA-132) and scrambled control siRNAs were 5′-GGUACUACUACGCCAGGUUTTAACCUGGCGUAGUAGUAC CTT-3′, and 5′-GCUUCUAGUACGCGAGGAUTTAUCCUCGCGU ACUAGAAGCTT-3′, respectively. After 24 hours, NHEK cells were treated with 10 μM 9(*S*)-HODE for 24 hours in the growth medium, and cell viability was determined using a CellTiter-Glo Luminescent Cell Viability Assay kit. To confirm the effects of siRNA, the levels of G2A mRNA 48 hours after transfection of siRNA were examined by a quantitative real-time RT-PCR analysis using the following primer set: sense primer, 5′-CATCCTCGTCGGGATCGTTC-3′; antisense primer, 5′-GAGAGAGGGATGGCAAAGCC-3′.

### Cell cycle analysis

NHEK cells were treated with 10 μM 9(*S*)-HODE or irradiated with 10 mJ cm$^{-2}$ UVB and then cultured in the growth medium. After 24 hours, cells were fixed with 70% ethanol and incubated with 250 μg ml$^{-1}$ RNase (Marligen Biosciences, Ijamsville, MD) in PBS containing 0.1% BSA at 37°C for 30 minutes. After staining with 50 μg ml$^{-1}$ propidium iodide (Sigma) on ice for 30 minutes, cell cycles were analyzed using an EPICS XL flow cytometer system.

### DNA fragmentation assay

NHEK cells were treated with 10 μM 9(*S*)-HODE or irradiated with 10 mJ cm$^{-2}$ UVB and then cultured in the growth medium. After 24 hours, cells were resuspended in lysis buffer (10 mM Tris-HCl, pH 7.4, 10 mM EDTA, and 0.5% Triton X100) and centrifuged for 5 minutes at 15,000 r.p.m. The resulting supernatants were collected and then incubated with 200 μg ml$^{-1}$ RNase at 37°C for 1 hour and 200 μg ml$^{-1}$ proteinase K at 50°C for 30 minutes. DNA was extracted with isopropanol, followed by agarose gel electrophoresis analysis.

### BrdU incorporation assay

NHEK cells were cultured in the basal medium for 2 hours and treated with 10 μM 9(*S*)-HODE in the growth medium for 18 hours. Amounts of incorporated BrdU were determined using a BrdU Labeling and Detection Kit III (Roche Applied Science) according to the manufacturer's instructions.

### UVB irradiation

Cells in PBS were irradiated with UVB using two FL20S/E lamps (Toshiba, Tokyo, Japan) that emitted most of their energy within the UVB range, with an emission peak at 306 nm. The strength of UVB rays was determined with a Model J-260 digital radiometer (Ultra-Violet Products, Cambridge, UK). Mock-irradiated cells were treated in an identical manner, except that they were shaded from the UVB lamps.

### Detection of ROS

HaCaT cells were loaded with 5 μM CM-$H_2$DCFDA (Molecular Probes) in PBS at 37°C for 20 minutes. After washing with PBS, cells were stimulated with increasing doses of UVB or 100 μM $H_2O_2$. Intracellular production of ROS was monitored at indicated times with a FLEX station scanning fluorometer system (Molecular Devices, Sunnyvale, CA) at an excitation wavelength of 485 nm and an emission wavelength of 525 nm.

### CONFLICT OF INTEREST

The authors state no conflict of interest.

## ACKNOWLEDGMENTS

We thank Ms Takeuchi Y. (Gunma University) for her expertise in immunohistochemistry, Dr Miyazaki J. (Osaka University) for providing the pCXN2.1 vector, and Drs Fusenig N.E. (German Cancer Research Center), Kuroki T. (University of Showa), and Nozawa Y. (Gifu International Institute of Biotechnology) for providing the HaCaT cells. This work was supported by Grants-in-Aid and the 21st Century Center of Excellence Program of the Ministry of Education, Culture, Sports, Science, and Technology of Japan.

## SUPPLEMENTARY MATERIAL

**Materials and Methods.** Detection of HODEs.

**Figure S1.** Involvement of G2A in cytokine secretion evoked by 9(*S*)-HODE in HaCaT cells.

**Figure S2.** Suppression of DNA synthesis and cell cycle arrest in the G0/1-phase by 9(*S*)-HODE in NHEK cells.

**Figure S3.** Production of 9-HODE by UVB and $H_2O_2$.

## REFERENCES

Baer AN, Costello PB, Green FA (1990) Free and esterified 13(R,S)-hydroxyoctadecadienoic acids: principal oxygenase products in psoriatic skin scales. *J Lipid Res* 31:125–30

Baer AN, Costello PB, Green FA (1991) Stereospecificity of the products of the fatty acid oxygenases derived from psoriatic scales. *J Lipid Res* 32: 341–7

Bayer M, Mosandl A, Thaci D (2005) Improved enantioselective analysis of polyunsaturated hydroxy fatty acids in psoriatic skin scales using high-performance liquid chromatography. *J Chromatogr B Analyt Technol Biomed Life Sci* 819:323–8

Beckman JK, Bagheri F, Ji C, Blair IA, Marnett LJ (1994) Phospholipid peroxidation in tumor promoter-exposed mouse skin. *Carcinogenesis* 15:2937–44

Bickers DR, Athar M (2006) Oxidative stress in the pathogenesis of skin disease. *J Invest Dermatol* 126:2565–75

Boukamp P, Petrussevska RT, Breitkreutz D, Hornung J, Markham A, Fusenig NE (1988) Normal keratinization in a spontaneously immortalized aneuploid human keratinocyte cell line. *J Cell Biol* 106:761–71

Caricchio R, McPhie L, Cohen PL (2003) Ultraviolet B radiation-induced cell death: critical role of ultraviolet dose in inflammation and lupus autoantigen redistribution. *J Immunol* 171:5778–86

Chiba H, Michibata H, Wakimoto K, Seishima M, Kawasaki S, Okubo K *et al.* (2004) Cloning of a gene for a novel epithelium-specific cytosolic phospholipase A2, cPLA2delta, induced in psoriatic skin. *J Biol Chem* 279:12890–7

Godessart N, Camacho M, Lopez-Belmonte J, Anton R, Garcia M, de Moragas JM *et al.* (1996) Prostaglandin H-synthase-2 is the main enzyme involved in the biosynthesis of octadecanoids from linoleic acid in human dermal fibroblasts stimulated with interleukin-1beta. *J Invest Dermatol* 107:726–32

Gron B, Iversen L, Ziboh V, Kragballe K (1993a) Distribution of monohydroxy fatty acids in specific human epidermal phospholipids. *Exp Dermatol* 2:38–44

Gron B, Iversen L, Ziboh V, Kragballe K (1993b) Monohydroxy fatty acids esterified to phospholipids are decreased in lesional psoriatic skin. *Arch Dermatol Res* 285:449–54

Grone A (2002) Keratinocytes and cytokines. *Vet Immunol Immunopathol* 88:1–12

Grossman RM, Krueger J, Yourish D, Granelli-Piperno A, Murphy DP, May LT *et al.* (1989) Interleukin 6 is expressed in high levels in psoriatic skin and stimulates proliferation of cultured human keratinocytes. *Proc Natl Acad Sci USA* 86:6367–71

Heck DE, Vetrano AM, Mariano TM, Laskin JD (2003) UVB light stimulates production of reactive oxygen species: unexpected role for catalase. *J Biol Chem* 278:22432–6

Ichihashi M, Ueda M, Budiyanto A, Bito T, Oka M, Fukunaga M *et al.* (2003) UV-induced skin damage. *Toxicology* 189:21–39

Kabarowski JH, Zhu K, Le LQ, Witte ON, Xu Y (2001) Lysophosphatidylcholine as a ligand for the immunoregulatory receptor G2A. *Science* 293: 702–5

Kulke R, Bornscheuer E, Schluter C, Bartels J, Rowert J, Sticherling M *et al.* (1998) The CXC receptor 2 is overexpressed in psoriatic epidermis. *J Invest Dermatol* 110:90–4

Kulke R, Todt-Pingel I, Rademacher D, Rowert J, Schroder JM, Christophers E (1996) Co-localized overexpression of GRO-alpha and IL-8 mRNA is restricted to the suprapapillary layers of psoriatic lesions. *J Invest Dermatol* 106:526–30

Le LQ, Kabarowski JH, Weng Z, Satterthwaite AB, Harvill ET, Jensen ER *et al.* (2001) Mice lacking the orphan G protein-coupled receptor G2A develop a late-onset autoimmune syndrome. *Immunity* 14:561–71

Lehman TA, Rama M, Boukamp P, Stanek J, Bennett WP, Welsh JA *et al.* (1993) p53 mutations in human immortalized epithelial cell lines. *Carcinogenesis* 14:833–9

Lin P, Ye RD (2003) The lysophospholipid receptor G2A activates a specific combination of G proteins and promotes apoptosis. *J Biol Chem* 278:14379–86

Loftin CD, Eling TE (1996) Prostaglandin synthase 2 expression in epidermal growth factor-dependent proliferation of mouse keratinocytes. *Arch Biochem Biophys* 330:419–29

Marathe GK, Johnson C, Billings SD, Southall MD, Pei Y, Spandau D *et al.* (2005) Ultraviolet B radiation generates platelet-activating factor-like phospholipids underlying cutaneous damage. *J Biol Chem* 280: 35448–57

Marcelo CL, Duell EA, Rhodes LM, Dunham WR (1992) *In vitro* model of essential fatty acid deficiency. *J Invest Dermatol* 99:703–8

McKenzie RC, Sauder DN (1990) The role of keratinocyte cytokines in inflammation and immunity. *J Invest Dermatol* 95:105S–7S

Moch D, Schewe T, Kuhn H, Schmidt D, Buntrock P (1990) The linoleic acid metabolite 9DS-hydroxy-10,12(E,Z)-octadecadienoic acid is a strong proinflammatory mediator in an experimental wound healing model of the rat. *Biomed Biochim Acta* 49:201–7

Murakami N, Yokomizo T, Okuno T, Shimizu T (2004) G2A is a proton-sensing G-protein-coupled receptor antagonized by lysophosphatidylcholine. *J Biol Chem* 279:42484–91

Nagy L, Tontonoz P, Alvarez JG, Chen H, Evans RM (1998) Oxidized LDL regulates macrophage gene expression through ligand activation of PPARgamma. *Cell* 93:229–40

Obinata H, Hattori T, Nakane S, Tatei K, Izumi T (2005) Identification of 9-hydroxyoctadecadienoic acid and other oxidized free fatty acids as ligands of the G protein-coupled receptor G2A. *J Biol Chem* 280: 40676–83

Ohta Y, Katayama I, Funato T, Yokozeki H, Nishiyama S, Hirano T *et al.* (1991) *In situ* expression of messenger RNA of interleukin-1 and interleukin-6 in psoriasis: interleukin-6 involved in formation of psoriatic lesions. *Arch Dermatol Res* 283:351–6

Radu CG, Nijagal A, McLaughlin J, Wang L, Witte ON (2005) Differential proton sensitivity of related G protein-coupled receptors T cell death-associated gene 8 and G2A expressed in immune cells. *Proc Natl Acad Sci USA* 102:1632–7

Rivier M, Safonova I, Lebrun P, Griffiths CE, Ailhaud G, Michel S (1998) Differential expression of peroxisome proliferator-activated receptor subtypes during the differentiation of human keratinocytes. *J Invest Dermatol* 111:1116–21

Schroder JM, Gregory H, Young J, Christophers E (1992) Neutrophil-activating proteins in psoriasis. *J Invest Dermatol* 98:241–7

Terashi H, Izumi K, Rhodes LM, Marcelo CL (2000) Human stratified squamous epithelia differ in cellular fatty acid composition. *J Dermatol Sci* 24:14–24

Tuschil A, Lam C, Haslberger A, Lindley I (1992) Interleukin-8 stimulates calcium transients and promotes epidermal cell proliferation. *J Invest Dermatol* 99:294–8

Vicanova J, Weerheim AM, Kempenaar JA, Ponec M (1999) Incorporation of linoleic acid by cultured human keratinocytes. *Arch Dermatol Res* 291:405–12

Walterscheid JP, Ullrich SE, Nghiem DX (2002) Platelet-activating factor, a molecular sensor for cellular damage, activates systemic immune suppression. *J Exp Med* 195:171–9

Weng Z, Fluckiger AC, Nisitani S, Wahl MI, Le LQ, Hunter CA *et al.* (1998) A DNA damage and stress inducible G protein-coupled receptor blocks cells in G2/M. *Proc Natl Acad Sci USA* 95:12334–9

Westergaard M, Henningsen J, Svendsen ML, Johansen C, Jensen UB, Schroder HD *et al.* (2001) Modulation of keratinocyte gene expression and differentiation by PPAR-selective ligands and tetradecylthioacetic acid. *J Invest Dermatol* 116:702–12

Witte ON, Kabarowski JH, Xu Y, Le LQ, Zhu K (2005) Retraction. *Science* 307:206

Wright S (1991) Essential fatty acids and the skin. *Br J Dermatol* 125:503–15

Yoshizaki K, Nishimoto N, Matsumoto K, Tagoh H, Taga T, Deguchi Y *et al.* (1990) Interleukin 6 and expression of its receptor on epidermal keratinocytes. *Cytokine* 2:381–7

Rheumatology 2008;47:454–457
Advance Access publication 3 March 2008

doi:10.1093/rheumatology/ken058

Concise Report

# Mouse model of dermal fibrosis induced by one-time injection of bleomycin-poly(L-lactic acid) microspheres

Y. Shibusawa[1], I. Negishi[1], Y. Tabata[2] and O. Ishikawa[1]

**Objective.** Animal models are useful tools to study various aspects of human diseases. Bleomycin (BLM)-induced scleroderma mouse has been widely investigated as an animal model of scleroderma. Repeated injections of BLM, either daily or every other day, for 3–4 weeks are required to induce scleroderma in mice. Poly(L-lactic acid) (PLA) is a biodegradable, biocompatible and bioabsorbable device that has been widely investigated for controlled drug release. In this study, we fabricated BLM-containing PLA microspheres and subcutaneously injected them into C3H mice for only one time.

**Methods.** Treated skins were harvested at days 7 and 21. Then, histological examination and collagen content measurement assay were performed. The mRNA expression of $\alpha$1(I) collagen (COL1A1), monocyte chemoattractant protein-1 (MCP-1), TGF-$\beta_1$ and connective tissue growth factor (CTGF) were quantified by real-time PCR.

**Results.** Dermal fibrosis was histologically observed at day 7 after injection and remained present at day 21. Tissue responses against BLM-PLA microspheres alone were mild. Soluble collagen content and expression level of $\alpha$1(I) collagen mRNA were significantly elevated at day 21. Expression levels of MCP-1 mRNA and TGF-$\beta_1$ mRNA at day 7 and CTGF mRNA at day 21 were also elevated.

**Conclusion.** The present study demonstrated for the first time that one-time injection of BLM-PLA microspheres can induce dermal fibrosis in C3H mice. BLM-PLA microspheres thus offer a labour-saving, simple and powerful tool to establish an animal model of BLM-induced dermal fibrosis.

KEY WORDS: Bleomycin, Scleroderma, Mouse model, Dermal fibrosis, Drug delivery system, Poly(L-lactic acid).

## Introduction

SSc is a CTD characterized by extensive fibrosis associated with increased deposition of extracellular matrix (ECM) proteins in the skin and various internal organs, vascular injury and immunological abnormalities [1, 2]. To elucidate the pathogenesis and develop novel treatments, animal models are very valuable. As mouse models of systemic sclerosis, tight skin mouse, sclerodermatous graft-*versus*-host disease mouse and bleomycin (BLM)-induced skin fibrosis/scleroderma mouse have been extensively studied [3, 4]. Recent reports have described new murine models of scleroderma, involving injection of TGF-$\beta$ and connective tissue growth factor (CTGF) [5], a modified model of sclerodermatous graft-*versus*-host disease mouse [6] and relaxin gene knockout mouse [7].

Animal models of scleroderma induced by repeated subcutaneous injections of BLM have been established in various mouse strains [8]. These mice show dermal sclerosis comprising thickened and homogeneous collagen bundles, and pulmonary fibrosis. The present study established a simple and labour-saving method using poly(L-lactic acid) (PLA) microspheres containing BLM. This method requires a one-time injection of BLM, instead of repeated daily injections for 4 weeks.

## Materials and methods

### *Preparation of BLM-PLA microspheres*

PLA (molecular weight, 20 000) was purchased from Wako Pure Chemical Industries (Osaka, Japan). BLM was kindly supplied by Nippon Kayaku (Tokyo, Japan). PLA microspheres containing BLM were prepared by the solvent evaporation method with water-in-oil-in-water [(W/O)/W] emulsion [9]. Briefly, 200 µl of BLM dissolved in water was poured into 5 ml of methylene chloride containing 200 mg of PLA microspheres, followed by emulsifying probe sonication to form a W/O emulsion. The emulsion was added to 10 ml of a 1 wt% polyvinyl alcohol (PVA; weight-average molecular weight 90 000; polymerization degree 1800; degree of saponification, 88 mol%) solution saturated with methylene chloride at room temperature and agitated using a vortex mixer to form a (W/O)/W double emulsion. The double emulsion was stirred using an impeller (200 r.p.m.) at room temperature until methylene chloride was completely evaporated. Microspheres were collected by centrifugation (3700 g, 5 min, 4°C), washed three times with cold distilled water and finally lyophilized. For control, $H_2O$–PLA microspheres were prepared. To infer *in vivo* drug-release pattern, concentration of BLM incorporated in the microspheres and *in vitro* release from microspheres were measured with high-performance liquid chromatography as described [9]. All samples were run in triplicate.

### *BLM-PLA microsphere treatment*

For the next step, 0.5 mg of BLM-PLA microspheres containing 0.013 mg of BLM was suspended in 400 µl of PBS. Microspheres in phosphate-buffered saline (PBS) (400 µl) were subcutaneously injected into shaved back skin at one site of 8-week-old female C3H mice. Control mice were injected with control-PLA microspheres.

### *Histological examination*

Skin samples were fixed in 10% formalin solution and embedded in paraffin. Haematoxylin–eosin staining was performed on each section.

### *Collagen assay*

Soluble collagen content of skin was determined using a Sircol collagen assay kit (Biocolor, Belfast, UK) according to the instructions of the manufacturer.

[1]Department of Dermatology, Gunma University Graduate School of Medicine, Maebashi, Gunma and [2]Department of Biomaterials, Field of Tissue Engineering, Institute for Frontier Medical Sciences, Kyoto University, Sakyo-ku, Kyoto, Japan.

Submitted 11 October 2007; revised version accepted 24 January 2008.

Correspondence to: Y. Shibusawa, Department of Dermatology, Gunma University Graduate School of Medicine, 3-39-22 Showa-machi, Maebashi, Gunma, 371-8511, Japan. E-mail: yshibusa@showa.gunma-u.ac.jp